ChemComm

ROYAL SOCIETY OF CHEMISTRY

COMMUNICATION

View Article Online
View Journal | View Issue

Open Access Article. Published on 24 December 2021. Downloaded on 10/19/2025 4:37:06 AM.
This article is licensed under a Creative Commons Attribution-NonCommercial 3.0 Unported Licence.

Check for updates

Cite this: *Chem. Commun.*, 2022, **58**, 1338

Received 1st December 2021,
Accepted 23rd December 2021

DOI: 10.1039/d1cc06755a

rsc.li/chemcomm

Heteroatom oxidation controls singlet–triplet energy splitting in singlet fission building blocks†

J. Terence Blaskovits, Maria Fumanal, Sergi Vela, Yuri Cho and Clémence Corminboeuf *

Singlet fission (SF) is a promising multiexciton-generating process. Its demanding energy splitting criterion – that the S_1 energy must be at least twice that of T_1 – has limited the range of materials capable of SF. We propose heteroatom oxidation as a robust strategy to achieve sufficient S_1/T_1 splitting, and demonstrate the potential of this approach for intramolecular SF.

Singlet fission (SF) has shown potential to improve the power conversion efficiency in photovoltaic devices beyond the Shockly–Queisser limit by promoting the splitting of a photon-absorbing singlet exciton into two triplet excitons.[1] SF involves the excitation of a ground state (S_0) chromophore to an excited singlet state (S_1) upon absorption of light, followed by energy transfer to a second chromophore. The initial S_1 state is coupled to a triplet pair (^{1}TT) state, a process which may be mediated by low-lying charge transfer (CT) states or may proceed directly, *via* a resonance mechanism.[2,3] The triplet pair then evolves into physically separate and energetically independent triplets (T_1), one on each chromophore.

Among the requirements necessary for a system to be capable of SF, the most stringent is that the process be *thermodynamically* possible, meaning that the energy of the S_1 state must be no less than twice that of the T_1 state: $\Delta E_{ST} = E(S_1) - 2E(T_1) \geq 0$. This *energy splitting* term ΔE_{ST} is therefore the most relevant target property in the discovery of new SF materials.[1,4,5] It has been shown that (i) extending the conjugation, and increasing the (ii) biradicaloid[4] or (iii) quinoidal[6] character of a chromophore can improve ΔE_{ST}, as summarized in Scheme 1. These strategies have drawbacks. For instance, compounds with high diradicaloid and quinoidal character tend to suffer from chemical instability.[7]

A particular challenge arises in designing materials which fall into the $\Delta E_{ST} \geq 0$ regime: the S_1 and T_1 energies tend to move in parallel. When the excitation energies are stabilized to the point that ΔE_{ST} is fulfilled, T_1 is often too low to be of value for device applications. A historically relevant example of this is the acene family, in which the excited state energies decrease with an increasing number of fused rings. In early reports of SF, in anthracene (3 rings), SF was not favored due to a negative ΔE_{ST} and, therefore, the endothermicity of SF.[8] This was also the case for tetracene (4 rings),[9] while pentacene (5 rings) became the poster child for SF due to it being the first acene in which SF is exergonic ($\Delta E_{ST} > 0$), although its T_1 energy is already somewhat lower (0.9 eV) than desirable.[10] The next acene, hexacene,[11] exhibits much more favorable ΔE_{ST} for SF, but has a far too low T_1 energy (0.4 eV).

A moiety which stabilizes T_1 incrementally to the point that it can be tuned to remain above 1 eV (for exciton injection into silicon for instance, whose band gap is 1.1 eV) without also lowering S_1 substantially would be greatly beneficial (Scheme 1, right panel). Here, we identify a chemical functionality, heteroatom oxidation, which modulates the ΔE_{ST} in potential SF chromophores in a foreseeable way (Scheme 1 (iv)). This approach is motivated by the experimental observation that the oxidized form of thiophene (thiophene-*S*,*S*-dioxide) is an effective acceptor in donor–acceptor copolymers capable of intramolecular SF (iSF),[12–14] and that nitrone/*N*-oxide groups were found in large numbers in a recent screening of thousands

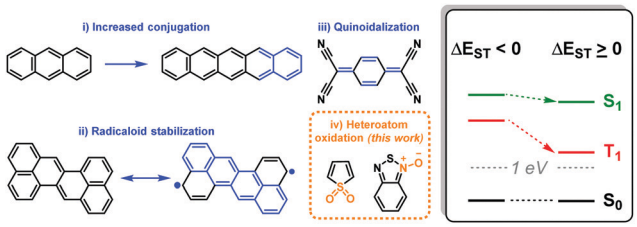

Scheme 1 Proposed strategies to increase singlet–triplet splitting (ΔE_{ST}) in organic chromophores.

Laboratory for Computational Molecular Design (LCMD), Institute of Chemical Sciences and Engineering (ISIC), École Polytechnique Fédérale de Lausanne (EPFL), CH-1015 Lausanne, Switzerland. E-mail: clemence.corminboeuf@epfl.ch

† Electronic supplementary information (ESI) available: Computational details, dataset, excited state energies for individual compounds, projected density of states, nucleus-independent chemical shifts. See DOI: 10.1039/d1cc06755a

This journal is © The Royal Society of Chemistry 2022

Open Access Article. Published on 24 December 2021. Downloaded on 10/19/2025 4:37:06 AM.
This article is licensed under a Creative Commons Attribution-NonCommercial 3.0 Unported Licence.

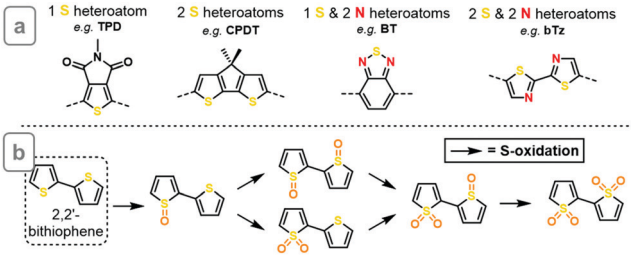

Scheme 2 (a) Examples of building blocks studied in this work. (b) Five oxidized derivatives of 2,2′-bithiophene.

of crystal structures for compounds with high ΔE_{ST}.[5] The present results show that, indeed, heteroatom oxidation governs the S_1 and T_1 energies and thus can be used to improve the singlet–triplet splitting of potential SF chromophores.

To establish if a systematic improvement in ΔE_{ST} can be achieved through heteroatom oxidation, we constructed a dataset consisting of 11 heteroatom-containing building blocks found widely in the organic electronics literature (see Fig. S1, ESI† for full dataset). These are classified by the number of heteroatoms in the conjugated system, as shown in Scheme 2a. All oxidized derivatives of these compounds were generated by placing one oxygen atom at the electron pair of all sp^2-hybridized nitrogen atoms, thereby forming *N*-oxide (nitrone) moieties, and one or two oxygen atoms at the electron pairs of all sulfur atoms, forming *S*-oxide or *S*,*S*-dioxide moieties, respectively (as shown for bithiophene in Scheme 2b). This produced a total of 67 oxidized compounds (all structures shown in ESI†). The oxidation of sp^3 nitrogens was not considered, as this would lead to charged or radical species. Compound geometries were relaxed using density functional theory (ωB97X-D/6-31G*), and the S_1 and T_1 exited-state energies were computed both vertically and at their minima using time-dependent DFT within the Tamm–Dancoff approximation at the same level of theory (see ESI† for details).

Representative results for the effect of oxidation on the vertical and adiabatic S_1, T_1 and ΔE_{ST} energies of bithiophene are shown in Fig. 1a and results for all other compounds are given in the ESI.† We observe a constant difference between the vertical and adiabatic excitation energies. This allows us to extend our previous observation in dimers[13] – that the adiabatic energy splitting cutoff ($\Delta E_{ST}^{adia} \geq 0$ eV) can be expressed as $\Delta E_{ST}^{vert} \geq -1$ eV in the Franck–Condon regime – to smaller (*monomer*) building blocks, due to the linear relationship between the two ΔE_{ST} values (Fig. S2, ESI†). Although it is immediately clear that increasing the number of oxygens (regardless of their position) stabilizes T_1 in an additive fashion across all compounds, the effect on S_1 is less evident. While mono-oxidation of sulfur leads to a sharp reduction in both S_1 and T_1 energies, which has little positive effect on ΔE_{ST}, a second oxidation of the same sulfur *increases* the S_1 energy while further stabilizing T_1, leading to a strong improvement in ΔE_{ST}. For example, the dioxide derivatives of bithiophene have $\Delta E_{ST}^{adia} \geq 0$ eV (above the grey line in Fig. 1a) while bare bithiophene and its mono-oxidized derivatives do not.

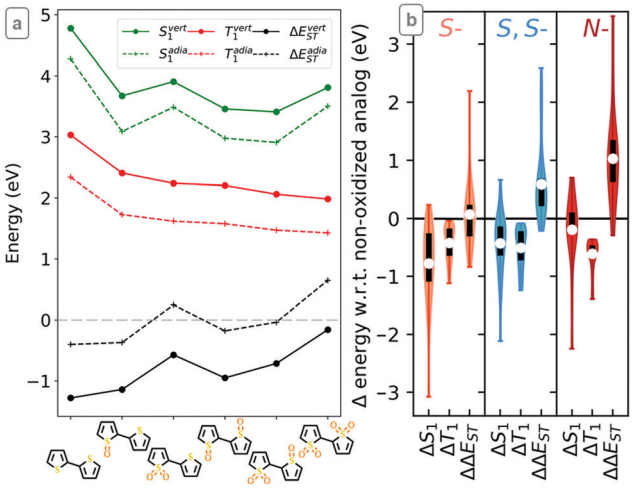

Fig. 1 (a) Vertical and adiabatic S_1, T_1, and ΔE_{ST} energies of bithiophene and its oxidized derivatives. Grey line indicates the ΔE_{ST} cut-off. (b) Summary of the change of adiabatic S_1, T_1, and ΔE_{ST} upon *S*-, *S*,*S*- and *N*-oxidation for all compounds, showing averages (white points), 1st–3rd quartiles (black bars), and maximal/minimal values (whiskers). See ESI† for details.

The same conclusions can be drawn with all other sulfur-containing units (Fig. S3–S6, ESI†): as outlined in Fig. 1b, single sulfur oxidations have little effect on ΔE_{ST} as they stabilize S_1 more than T_1, while double oxidations of sulfur are invariably beneficial to ΔE_{ST} due to their similar stabilization of T_1 but smaller impact on S_1. *N*-Oxidation systematically improves ΔE_{ST} through a robust stabilization of T_1 (Fig. S7 and S8, ESI†). These trends are observed regardless of the degree of oxidation of all others heteroatoms, resulting in a remarkably simple cumulative effect across all compounds: the most highly oxidized structures have the highest ΔE_{ST} of all combinations of oxidation products (Fig. 1 and Section S2 of ESI†).

To understand the effect of oxidation on S_1 and T_1 energies, we turned to the nature of the excitations in the simplest subunit, thiophene (Table 1). The T_1 state of thiophene is dominated by a local HOMO → LUMO transition in the carbon backbone, while the S_1 state involves predominantly charge transfer (CT) from sulfur (HOMO−1) into the backbone.

Table 1 Excitation energies, character and molecular orbitals most involved in excitations for thiophene (Th), thiophene-*S*-oxide (Th-1O) and thiophene-*S*,*S*-dioxide (Th-2O). Atoms involved in orbitals contributing to CT character are highlighted in green. BB = carbon backbone. Orbitals shown in Fig. S11 (ESI)

Compound		State	State character	Orbitals	E (eV)	ΔE_{vert}^{ST} (eV)
	Th	T_1	Local BB	H → L	3.90	−1.47
		S_1	CT S-to-BB	H−1 → L	6.33	
	Th-1O	T_1	Local BB	H−1 → L	3.01	−2.24
		S_1	CT O-to-BB	H → L	3.78	
	Th-2O	T_1	Local BB	H → L	2.80	−0.94
		S_1	Local BB	H → L	4.66	

Open Access Article. Published on 24 December 2021. Downloaded on 10/19/2025 4:37:06 AM.
This article is licensed under a Creative Commons Attribution-NonCommercial 3.0 Unported Licence.

In thiophene-*S*-oxide, the T_1 excitation is a localized HOMO−1 → LUMO transition on the backbone, as the HOMO is located on the oxygen. It is instead the S_1 excitation which corresponds to a HOMO → LUMO CT state from oxygen into the backbone π* orbital, which explains the significant stabilization of S_1 upon mono-oxidation. Finally, in thiophene-*S*,*S*-dioxide both S_1 and T_1 are characterized by backbone HOMO → LUMO (π → π*) transitions, as the O and S orbitals are much lower in energy.

Similarly, in benzodithiophenedione (BDO) and thienopyrroledione (TPD, see Fig. S12, ESI†), S_1 is stabilized by CT states from the oxygen *n* orbitals into the π* orbital of the backbone. The difference compared to thiophene is that BDO and TPD already contain oxygens in their conjugated systems by virtue of their carbonyls, such that S_1 in non-oxidized TPD and BDO is described by CT from the carbonyls into the heterocycle. A first *S*-oxidation stabilizes S_1 through CT from the S═O moiety, as with thiophene-*S*-oxide, while a second oxidation shifts the source of CT back to the carbonyls. Therefore, the *nature* of the CT (*i.e.* the *n* orbitals involved) changes, depending on the structure of the unit, but the stabilizing effect of a single *S*-oxidation on S_1 remains constant across all compounds. And yet, the oscillator strength of S_1 tends to drop significantly for *S*-mono-oxidized compounds (see Fig. S14, ESI†), which may have consequences on the SF decay pathway and overall mechanism.[15] Less impact is expected on the photophysical properties of the S_1 state of *S*,*S*- and *N*-oxidized compounds.

Recent work has rationalized ΔE_{ST} based on ground- and excited-state aromaticity.[16,17] To explain the effect of these substitutions on aromaticity, we computed the nucleus independent chemical shifts (NICS) of thiophene, TPD, and thiazole (Fig. S15, ESI†). While thiophene is aromatic in the ground state and anti-aromatic in the first triplet state, thiophene-*S*-oxide is much less aromatic in the ground state, but still significantly anti-aromatic in the triplet. The absence of lone pairs on the sulfur atom of thiophene-*S*,*S*-dioxide leads to non-aromatic character of both the ground state singlet and first triplet. This is reflected in the bond order of the backbone which, like butadiene, is reversed in the triplet (CH–CH═CH–CH) compared to the singlet (CH═CH–CH═CH). This is not the case for non-oxidized or mono-oxidized thiophene (Fig. S16, ESI†). The TPD ring aromaticity is similarly suppressed upon the double oxidation of sulfur. Put together, these results suggest that the destabilization of S_1 upon *S*,*S*-dioxidation, and its consequently beneficial effect on ΔE_{ST}, originate from the SO_2 moiety eliminating the aromatic character of the heterocycle and instead inducing a polarized butadiene-like behavior to the backbone.[18] In this way, T_1 is sufficiently stabilized, while the stabilizing effect of CT from S (in thiophene rings) or O (in thiophene-*S*-oxide rings) into the π-system observed in S_1 is eliminated. This is similar to the 'breaking' of conjugation in polycyclic hydrocarbons through boron-doping, an approach proposed to build molecules that fulfill ΔE_{ST}.[19]

CT, primarily from oxygen into sulfur (HOMO → LUMO+1), also accounts for the stabilization of S_1 in *N*-oxidized benzothiadiazole (BT, see Fig. S13, ESI†), compared to non-oxidized BT, which has a local π → π* (HOMO → LUMO) character. The T_1 states are also described by a π → π* transition in both non-oxidized and *N*,*N*′-dioxidized BT. The inclusion of the N–O moiety in the conjugated system reduces the π/π* energy gap, leading to an extreme lowering of both the S_1 and T_1 energies by approximately 2 eV. *N*-Oxidation has the effect of strongly reducing the antiaromatic character of the triplet (Fig. S15, ESI†), while retaining ground state aromaticity, explaining the significant T_1 stabilization and consequent increase in ΔE_{ST}.

iSF has been demonstrated experimentally in donor–acceptor (D–A) polymers,[12,20,21] in which the triplet pair formation is mediated through low-lying donor-to-acceptor CT states, while the spatial separation of the acceptors by the absorbing donor leads to a weakly bound ^{1}TT state. We have recently proposed a protocol with which to identify potential polymer candidates for iSF based on the ΔE_{ST} of the constituent monomers and their relative frontier molecular orbital (FMO) energies.[13,14] To assess the performance of these new oxidized units to form iSF-capable D–A pairs, we treat all those in the dataset that fulfill $\Delta E_{ST}^{adia} \geq 0$ (and $\Delta E_{ST}^{vert} \geq -1$ eV, *vide supra*) as *acceptor* monomers (34 compounds). The FMOs of each acceptor were compared to all other buildings blocks (2244 monomer pairs), and only those whose FMO arrangement is conducive to CT (*i.e.* donor HOMO higher than acceptor HOMO and donor LUMO higher than acceptor LUMO; see earlier work for details[14]) were retained. For these 631 D–A combinations, the dimers were generated, their ground state geometries optimized, and their vertical excited states were evaluated at the same level of theory as the monomers. All dimers exhibit energy splitting above the vertical threshold $\Delta E_{ST}^{vert} \geq -1$ eV (Fig. S17, ESI†), which is consistent with our observation[14] that the dimer ΔE_{ST} originates from the monomer with the higher (*i.e.* more positive) ΔE_{ST}.

We have previously outlined two other requirements beyond ΔE_{ST} for iSF to be possible in D–A systems: S_1 must have significant donor-to-acceptor CT character to drive triplet-pair formation ($S_1 \rightarrow {}^1$TT), and T_1 must be located on the acceptor to promote dissociation of the triplet states (^{1}TT → $T_1 + T_1$).[13,14] Deactivation of S_1 towards higher energy triplet states is

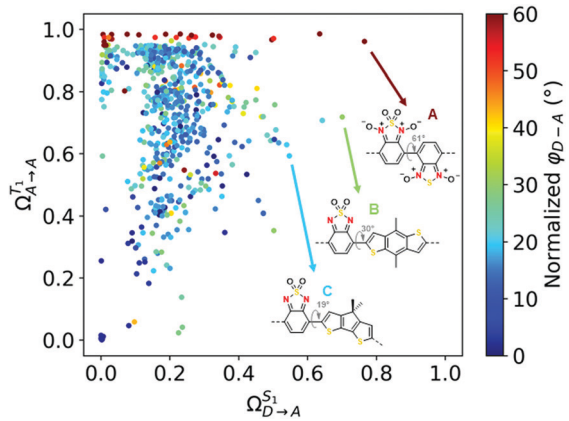

Fig. 2 Donor-to-acceptor charge-transfer character of S_1 ($\Omega^{S1}_{D\rightarrow A}$, *x*-axis) and local acceptor character of T_1 ($\Omega^{T1}_{A\rightarrow A}$, *y*-axis) in dimers, colored by the dihedral between the donor and acceptor (φ_{D-A}).

Open Access Article. Published on 24 December 2021. Downloaded on 10/19/2025 4:37:06 AM.
This article is licensed under a Creative Commons Attribution-NonCommercial 3.0 Unported Licence.

neglected but the $S_1 \rightarrow {}^1TT$ transition required for iSF is expected to be the most efficient decay pathway (see Section S6). Quantum chemical descriptors were introduced to quantify these criteria using the character of excited states (see ESI†). Fig. 2 shows the fraction of CT from donor to acceptor in S_1 ($\Omega^{S1}_{D\rightarrow A}$) and the fraction of local T_1 character on the acceptor ($\Omega^{T1}_{A\rightarrow A}$). The upper righthand corner corresponds to the 'ideal' region in which these two criteria are fulfilled simultaneously. The majority of the present dimers display a highly localized T_1 ($\Omega^{T1}_{A\rightarrow A}$ = 0.5–1.0) and non-negligible S_1 CT character ($\Omega^{S1}_{D\rightarrow A}$ = 0.1–0.4), but are nonetheless not in the ideal region.

A striking exception are dimers containing *N*,*N*-dioxidized benzothiadiazole along the top of Fig. 2, indicating pure localization of T_1 on the acceptor (Fig. S17, ESI†). In addition to stabilizing T_1 to achieve positive ΔE_{ST}, this acceptor induces dihedral torsion to the D–A linkage ($\varphi_{D-A} \approx 50^\circ$), thereby contributing to very high CT in S_1 (up to 0.8). The best of these dimers is shown in Fig. 2 (compound A), and is revealed to have a donor partner which differs from the acceptor only with regard to the sulfur oxidation. However, the *N*-oxidation of compound A stabilizes T_1 too much for it to be of practical use if extracted (0.41 eV). All other dimers constructed with this acceptor suffer from this problem (T_1 = 0.3–0.9 eV). Two other dimers (B and C) have a similar acceptor, albeit without *N*-oxidation, which leads to promising excited state behavior in the dimer and appropriate ΔE_{ST} (as with A), but importantly, they retain attractive T_1 energies (1.47 eV and 1.24 eV, respectively; see Table S2, ESI†). The absence of nitroxides leads to smaller dimer dihedrals (30° and 19°) and therefore slightly lower CT compared to A, but are still near the ideal region. This analysis demonstrates that through judicious chromophore oxidation, both ΔE_{ST} and T_1 can be fine-tuned without losing the CT character which mediates the SF process in D–A copolymers.

We have disclosed heteroatom oxidation as a convenient handle through which to modulate singlet–triplet splitting in SF building blocks. Beneficial ΔE_{ST} through double oxidation of sulfur is obtained by suppressing aromaticity while maintaining overall conjugation, thereby stabilizing T_1 compared to non-oxidized analogs, while having a smaller impact on S_1. A higher number of heteroatom oxidations stabilizes T_1 additively, making it possible to drive the T_1 energy down as far as necessary to achieve exergonic splitting. The utility of this approach is demonstrated using new *S*- and *N*-oxidized compounds to construct D–A materials for iSF, although this method is equally valid in intermolecular SF materials design. D–A systems based on a new benzothiadiazole-*S*,*S*-dioxide acceptor may be excellent candidates, as sulfur oxidation modulates the excited state energies for SF to be thermodynamically possible while ensuring that the resulting T_1 is appropriate for injection into silicon (1.1–1.7 eV). *N*-Oxidations, on the other hand, also systematically improve ΔE_{ST}, but at the expense of an attractive T_1 energy. While these specific units have not been described in the literature, previously reported preparation of *S*-oxidized[22] and *S*,*S*-(di)oxidized[22,23] analogs of benzothiadiazole, as well as *N*-oxidized thiazoles,[24] bithiazoles,[25] and thiadiazoles[26] suggest that they are synthesizable.

The authors are grateful to the EPFL for financial support. M. F. acknowledges funding from European Union's H2020 research and innovation, under MSCA-IF-2018 (G.A. #836849).

Conflicts of interest

There are no conflicts to declare.

References

1 M. B. Smith and J. Michl, *Chem. Rev.*, 2010, **110**, 6891–6936.
2 E. G. Fuemmeler, S. N. Sanders, A. B. Pun, E. Kumarasamy, T. Zeng, K. Miyata, M. L. Steigerwald, X.-Y. Zhu, M. Y. Sfeir and L. M. Campos, *ACS Cent. Sci.*, 2016, **2**, 316–324.
3 D. Casanova, *Chem. Rev.*, 2018, **118**, 7164–7207.
4 I. Paci, J. C. Johnson, X. Chen, G. Rana, D. Popović, D. E. David, A. J. Nozik, M. A. Ratner and J. Michl, *J. Am. Chem. Soc.*, 2006, **128**, 16546–16553.
5 D. Padula, Ö. H. Omar, T. Nematiaram and A. Troisi, *Energy Environ. Sci.*, 2019, **12**, 2412–2416.
6 B. C. Streifel, J. L. Zafra, G. L. Espejo, C. J. Gómez-García, J. Casado and J. D. Tovar, *Angew. Chem., Int. Ed.*, 2015, **54**, 5888–5893.
7 Z. Zeng, X. Shi, C. Chi, J. T. López Navarrete, J. Casado and J. Wu, *Chem. Soc. Rev.*, 2015, **44**, 6578–6596.
8 S. Singh and B. Stoicheff, *J. Chem. Phys.*, 1963, **38**, 2032–2033.
9 C. E. Swenberg and W. T. Stacy, *Chem. Phys. Lett.*, 1968, **2**, 327–328.
10 S. Yoo, B. Domercq and B. Kippelen, *Appl. Phys. Lett.*, 2004, **85**, 5427–5429.
11 N. R. Monahan, D. Sun, H. Tamura, K. W. Williams, B. Xu, Y. Zhong, B. Kumar, C. Nuckolls, A. R. Harutyunyan, G. Chen, H.-L. Dai, D. Beljonne, Y. Rao and X. Y. Zhu, *Nat. Chem.*, 2017, **9**, 341–346.
12 E. Busby, J. Xia, Q. Wu, J. Z. Low, R. Song, J. R. Miller, X. Zhu, L. M. Campos and M. Y. Sfeir, *Nat. Mater.*, 2015, **14**, 426.
13 J. T. Blaskovits, M. Fumanal, S. Vela and C. Corminboeuf, *Chem. Mater.*, 2020, **32**, 6515–6524.
14 J. T. Blaskovits, M. Fumanal, S. Vela, R. Fabregat and C. Corminboeuf, *Chem. Mater.*, 2021, **33**, 2567–2575.
15 M. Fumanal and C. Corminboeuf, *J. Phys. Chem. Lett.*, 2021, **12**, 7270–7277.
16 O. El Bakouri, J. R. Smith and H. Ottosson, *J. Am. Chem. Soc.*, 2020, **142**, 5602–5617.
17 K. J. Fallon, P. Budden, E. Salvadori, A. M. Ganose, C. N. Savory, L. Eyre, S. Dowland, Q. Ai, S. Goodlett and C. Risko, *J. Am. Chem. Soc.*, 2019, **141**, 13867–13876.
18 M. M. Oliva, J. Casado, J. T. L. Navarrete, S. Patchkovskii, T. Goodson, M. R. Harpham, J. S. Seixas de Melo, E. Amir and S. Rozen, *J. Am. Chem. Soc.*, 2010, **132**, 6231–6242.
19 J. Stoycheva, A. Tadjer, M. Garavelli, M. Spassova, A. Nenov and J. Romanova, *J. Phys. Chem. Lett.*, 2020, **11**, 1390–1396.
20 G. Grancini, M. Maiuri, D. Fazzi, A. Petrozza, H. Egelhaaf, D. Brida, G. Cerullo and G. Lanzani, *Nat. Mater.*, 2013, **12**, 29.
21 J. Hu, K. Xu, L. Shen, Q. Wu, G. He, J.-Y. Wang, J. Pei, J. Xia and M. Y. Sfeir, *Nat. Commun.*, 2018, **9**, 2999.
22 T. Linder, E. Badiola, T. Baumgartner and T. C. Sutherland, *Org. Lett.*, 2010, **12**, 4520–4523.
23 D. Pinkowicz, Z. Li, P. Pietrzyk and M. Rams, *Cryst. Growth Des.*, 2014, **14**, 4878–4881.
24 E. Amir and S. Rozen, *Chem. Commun.*, 2006, 2262–2264.
25 R. A. Mirabal, L. Vanderzwet, S. Abuadas, M. R. Emmett and D. Schipper, *Chem. – Eur. J.*, 2018, **24**, 12231–12235.
26 L. S. Konstantinova, E. A. Knyazeva, N. V. Obruchnikova, Y. V. Gatilov, A. V. Zibarev and O. A. Rakitin, *Tetrahedron Lett.*, 2013, **54**, 3075–3078.